ELSEVIER

Chemical Physics 226 (1998) 337–349

Chemical Physics

Self-assembly of alkylsiloxane monolayers on fused silica studied by XPS and sum frequency generation spectroscopy

A.S. Lagutchev [a,1], K.J. Song [a,*], J.Y. Huang [b], P.K. Yang [b], T.J. Chuang [a]

[a] *Institute of Atomic and Molecular Sciences, Academia Sinica, P.O. Box 23-166, Taipei 10764, Taiwan*
[b] *Institute of Electro-Optical Engineering, National Chiao-Tung University, Hsinchu, Taiwan*

Received 14 March 1997

Abstract

Infrared–visible sum frequency generation (SFG) vibrational spectroscopy in the C–H stretching region was used to study a set of self-assembled monolayers, formed from octyltrichlorosilane [$CH_3(CH_2)_7SiCl_3$], its partially fluorinated analog, (tridecafluoro-1,1,2,2-tetrahydrooctyl)-1-trichlorosilane [CF_3-$(CF_2)_5(CH_2)_2SiCl_3$] and their mixtures. SFG measurements were complemented with transmission–absorption FTIR spectroscopy and X-ray photoemission spectroscopy. Simultaneous self-assembly of both chlorosilanes results in preferential deposition of the fluorinated compound. The major reason for this behavior is the alkyl chain fluorination. There is a strong spectroscopic evidence of close coadsorption of fluorinated and non-fluorinated molecules in mixed monolayers. It follows that the species in self-assembled monolayers of binary composition do not segregate into different phases as it is observed for similar Langmuir–Blodgett films. Distinct differences found in SFG spectra of fluorinated and non-fluorinated samples indicate that SFG spectroscopy is much more sensitive than FTIR in detection of symmetry distortions in the alkyl chain of the amphiphiles. Both SFG and FTIR spectroscopic data show the presence of hydrocarbon residue in fluorinated and mixed films that is very likely due to hexadecane used as a solvent during monolayer deposition. © 1998 Elsevier Science B.V.

1. Introduction

Recent interest in solid lubricants [1] and tribological problems in general has initiated studies of various types of organic thin films [2]. Alkylchlorosilane molecules consisting of chlorosilane head group attached to an alkyl chain can adsorb by covalent bonding on OH-terminated surface forming cross-linked alkylsiloxane monolayer. This kind of organosilane adsorption is usually irreversible. The resulting film demonstrates high chemical, thermal and mechanical stability [3–5]. The important feature of alkylsilane adsorption is its ability to self-assemble on a surface from the solution in a form of compact monolayer, which is attractive for potential technological applications. Consequently, such monomolecular films have become the subject of extensive investigation [5–8] since the first successful depositions [9,10]. Self-assembled alkylsiloxane films, being technically easy to deposit, can provide desired modification of friction [11], adhesion [12], wettability [13] and other surface characteristics. Crystalline quartz, fused silica, glass, mica, oxidized

* Corresponding author. E-mail: song@po.iams.sinica.edu.tw.
[1] E-mail: lagutch@aries.scs.uiuc.edu.

PII S0301-0104(97)00263-2

silicon and many other hydrophilic polar surfaces can serve as convenient substrates for alkylsiloxane self-assembled films. Owing to the unique properties of the fluorinated hydrocarbon polymers, considerable effort has been invested in recent years in the investigation of various monolayers with fluorinated alkyl chains in general [14,15] and fluorinated alkylsiloxanes in particular [3,16–18].

The variety of adsorbate–substrate pairs suitable for self-assembled layer formation is, however, not very wide (compared, for instance, with those suitable for Langmuir–Blodgett deposition). As a result, during the very first attempts to produce self-assembled monolayers (SAM), significant effort was devoted either to subsequent chemical modification [9] or to growing layers of mixed composition [10] to achieve desired surface properties.

The goal of the current study was the investigation of the mixed SAMs self-assembly. Ordinary, fluorinated and mixed alkylsiloxane self-assembled monolayers were formed on fused silica surface from hexadecane solution. Two investigated siloxanes had the same chain length and were deposited either under identical conditions or in a mixture. This, to our knowledge, has never been done before by self-assembly. However, similar monolayers were prepared and investigated by Ge et al. [3] using the Langmuir–Blodgett technique. This gives us a possibility to compare the results of two different film preparation methods.

The main experimental technique applied was IR–visible sum frequency generation spectroscopy (SFG). This technique as first demonstrated by Shen and coworkers [19–21] is in fact a sophisticated method of vibrational spectroscopy at surfaces or material interfaces. An IR pulse excites a molecular vibration in the adlayer, while a synchronous visible pulse shifts the response to the visible region by non-linear frequency summation. Vibrational spectrum is recorded by scanning IR frequency across the resonance. With SFG, it is possible to obtain information about the orientation of molecules on the surface, from the different polarization combinations of incident IR and visible pulse and the detected sum frequency. Only those transitions that are both IR and Raman active can contribute to sum frequency signal. We intend to demonstrate here that this specific selection rule can provide a possibility to detect symmetry distortions of the adsorbed molecules, which are not revealed by either IR or Raman spectroscopy.

The SFG signal is proportional to the square magnitude of the effective surface susceptibility $\chi_s^{(2)}$, which in turn is proportional to the surface density of the adsorbed molecules $\chi_s^{(2)}$ can be represented as a sum of resonant and non-resonant contributions [19], thus

$$l(\omega_{sf}) \propto |\chi_s^{(2)}(\omega_{sf}, \omega_1, \omega_2)|^2 = \left| \chi_{nr}^{(2)} + \sum_q \frac{A_q}{(\omega_1 - \omega_q + i\gamma_q)} \right|^2 \quad (1)$$

Here A_q, ω_q and γ_q stand for amplitude, frequency and damping constant of qth normal mode; ω_{sf}, ω_1 and ω_2 are sum, IR and visible excitation frequencies, respectively; $\chi_{nr}^{(2)}$ is the non-resonant part of the surface second order susceptibility. To provide direct link to surface concentration, SFG spectra in this paper are expressed (unless specified otherwise) in terms of a square root of detected SFG light intensity. i.e. the magnitude of $\chi^{(2)}$ which is referred to as 'SFG strength'.

The main advantage of SFG technique for surface analysis comes from the inability of many substrates to generate sum frequency in the bulk, which is true for all centrosymmetric media in electro–dipole approximation. This feature allows elimination of bulk contribution in the response and makes possible the observation of weak signals originating only from the adlayer. Also, very weak signals from the samples with low surface concentration can be measured by photon counting in the visible region. The methyl and methylene stretching modes of alkylsiloxane monolayers appear in the 2800–3000 cm^{-1} frequency region and the required tunable infrared radiation for SFG measurements can be conveniently generated by a $LiNbO_3$ parametric oscillator.

Another advantage of SFG for investigation of alkylsiloxane monolayers comes from the fact that the resonant part of $\chi^{(2)}$ is an orientational average over adsorbed molecules [22]. As a result, only the ordered part of the film is capable of generating SFG signal. This is especially useful for fluorinated samples that were reported to contain some amorphous residue of silane hydrolysis products [18], despite all

efforts to suppress such hydrolysis in the bulk solution during film deposition.

Standard FTIR transmission–absorption spectroscopy and X-ray photoemission spectroscopy (XPS) measurements were also performed in our study for comparison.

2. Experimental

Two major types of alkylsiloxane monolayers (in both pure and mixed states) were investigated. These were produced from octyltrichlorosilane (CH_3-$(CH_2)_7$-$SiCl_3$) and its fluorinated derivative, (tridecafluoro-1,1,2,2-tetrahydrooctyl)-1-trichlorosilane (CF_3-$(CF_2)_5$-$(CH_2)_2$-$SiCl_3$). Fluorination of the latter silane was incomplete as two methylene groups were still present next to the silicon atom in otherwise fluorinated alkyl chain. It is known that such comparatively short-chain silanes often form more disordered and less compact [5,23] SAMs than the long chain silanes. However, our choice was limited by the availability of fluorinated compound and the requirement of similar chain length for consistent comparison. During adsorption, alkylsilanes are believed [24] to be hydrolyzed by residual water present in the bulk solvent and on the surface, exchanging chlorine atoms with OH groups and later form siloxane (Si–O–Si) bonds with underlying substrate and between each other. Alkylsiloxane monolayers produced from octyltrichlorosilane and its fluorinated derivative are referred here as C8H and C8F, respectively. For studying chain-length effects, we also prepared some samples from octadecyltrichlorosilane (OTS), which has been the most widely studied source of alkylsiloxane monolayers. The sample is referred to as C18H. All silanes were purchased from Petrach Systems and used without further purification.

Alkylsiloxane monolayer samples were prepared generally following the procedure described by Parikh et al. [25]. Fused silica substrates were cleaned by etching in piranha solution (H_2SO_4:H_2O_2 = 1:4) for 1/2 h and then were kept in ozone atmosphere until deposition. For deposition the samples were dipped into 2.5 mM solutions of octyltrichlorosilane, its fluorinated analog or OTS for 20 minutes. Pure hexadecane (Aldrich) or 80:20 hexadecane:carbon tetrachloride volume mixture was used as a solvent. For the preparation of mixed monolayers, the above mentioned solutions were mixed in different volume proportions, while maintaining the same molar concentration. After deposition, the samples were rinsed in carbon tetrachloride and ethanol and then baked for 2 h at 100°C. The latter procedure was reported [16] to facilitate rigid cross-linking of the monolayers. Traces of the organic residue, originating probably from partial hydrolysis and polymerization of active compounds during deposition, were later removed by wiping if necessary.

The SFG spectrometer consisted of a tunable infrared light source based on $LiNbO_3$ parametric oscillator and a LBO frequency doubler as the visible light source (532 nm). Both were pumped by a Continuum PY61C Nd:Yag mode-locked laser with 35 ps pulse width and 20 Hz repetition rate. Effective IR tuning range was 2400–3600 cm^{-1}, thus C–H stretching region was covered. Pulse energies at the sample surface were 0.2 and 1.5 mJ for IR and visible light, respectively. The IR beam was focused into less than 0.5 mm diameter spot, while visible light focusing was slightly less tight to avoid possible optical breakdown on the surface. Angles of incidence with respect to the surface normal were 45° and 37° for infrared and visible light, respectively. The frequency of tunable IR source was calibrated using standard polystyrene film samples. SFG spectra were recorded with various polarization (s and p) combinations of the incident light pulses and the sum frequency signal with respect to the plane of incidence. The *ssp*-polarization for the sum, visible and IR pulses, respectively, was employed most often because it produced the largest SFG signal. Unless specified otherwise, most spectra reported here were obtained with this polarization combination.

The emerging sum-frequency signal was filtered with a monochromator and then detected using a Hamamatsu R955 photomultiplier tube. The monochromator (Jobin Yvon H10, 1200 g/mm grating, 8 nm/mm linear dispersion, 1 mm slits) was adjusted synchronously with the tuning IR radiation frequency. 532 nm visible light scattered from the sample surface was suppressed first by spatial filtering and then by V-type holographic notch plus filter

(Kaiser Optical Systems) installed in front of the monochromator.

Infrared transmission–absorption spectra were recorded with Bomem MB-100 FTIR spectrometer, with 4 cm^{-1} resolution. The spectrometer was equipped with liquid nitrogen cooled InSb detector. Freshly ozone oxidized fused silica substrate was used as a reference.

The atomic content of the monolayers was checked by XPS using a VG-ESCA spectrometer, which was equipped with Mg Kα X-ray source and a CLAM-2 hemispherical energy analyzer. Photoemission very close to surface normal was detected in all experiments. Spectra were recorded with 1 eV step in 0–1000 eV region for survey scans and 0.1 eV step for narrow scans of individual element peaks. The instrument resolution checked with a gold sample was 1.2 eV. Due to insulating nature of fused silica substrate, a flood gun was employed to eliminate surface charging effects. Flood gun parameters were adjusted to maintain C(1s), Si(2p) and O(1s) binding energies close to 285, 103 and 533 eV, respectively. These numbers correspond to aliphatic carbon and SiO_2.

3. Results and discussion

3.1. Ordinary (non-fluorinated) samples

SFG spectra of all samples used in the present study show vibrational peaks in the 2800–3000 cm^{-1} region. Wide SFG scans performed in 2600–3400 cm^{-1} region show no additional features; in particular no OH stretches are detected. Also no trace of chlorine is observed by XPS, in general agreement with the mechanism of alkylsiloxane monolayer deposition [5]. In the 2800–3000 cm^{-1} region, symmetric and antisymmetric stretching modes of methyl (CH_3) and methylene (CH_2) groups can be identified. Alkyl chains consisting of methylene groups are believed to be nearly centrosymmetric [22] which makes their contribution to second order non-linear surface susceptibility $\chi_s^{(2)}$ very small. Thus, methylene C–H stretching modes should appear in SFG spectrum only if central symmetry of alkyl chains is distorted. In contrast to that, terminal methyl groups are clearly non-centrosymmetric and are easily detected with SFG, as in OTS monolayers investigated previously by Guyot-Sionnest et al. [26]. As expected, two peaks at methyl stretching frequencies appear in the SFG spectrum of C18H (OTS) monolayer (Fig. 1, solid squares). The peak at 2875 cm^{-1} arises from the symmetric stretch of CH_3, and the one at 2940 cm^{-1} was previously assigned to the Fermi resonance of symmetric CH_3 stretch and overtone of CH_3 bending mode [22]. These two peaks are also present in the spectrum of the shorter chain C8H monolayer (Fig. 1, open circles), but an additional peak at 2846 cm^{-1} and possibly a weak shoulder at 2920 cm^{-1} also appear. These features can be attributed to methylene symmetric and antisymmetric stretching modes. Their appearance shows that the shorter C8H alkyl chain is no longer centrosymmetric. Hoffmann et al. [23] have reported the increase in defects concentration with shortening of the alkyl chain of the monolayers. Methylene stretches were also shown to appear in SFG spectrum of OTS monolayer on glass due to increase of *trans–cis* defects concentration with increasing temperature [27]. Based on these results we attribute the appearance of methylene stretches in SFG spectra of C8H to the presence of *trans–cis* (*–gauche*) defects in this comparatively short-chain monolayer.

The infrared transmission–adsorption spectrum of C8H monolayer is shown in Fig. 2 (solid curve). The spectrum was recorded with 45° incidence and polar-

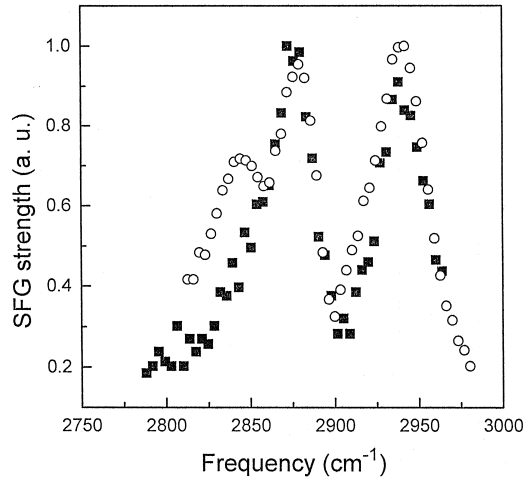

Fig. 1. SFG signal strengths for C18H (OTS) monolayer (solid squares), and C8H monolayer (open circles).

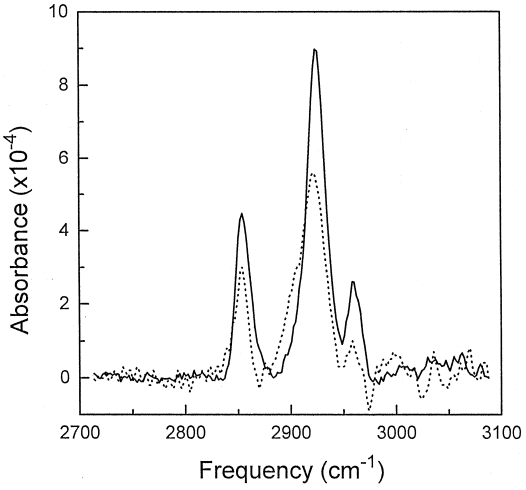

Fig. 2. IR transmission–absorption spectra of C8H (solid line) and C8F (dashed line) monolayers. 45° incident angle, *p*-polarization.

ization to maximize possible contribution from the methyl group. In contrast to SFG data, methylene features with symmetric and antisymmetric stretches at 2855 and 2925 cm^{-1} dominate in IR spectrum. Peak at 2960 cm^{-1} in C8H spectrum can be assigned to CH_3 antisymmetric vibration. The observed infrared spectrum is very similar to that of C18H (OTS) monolayer produced by Langmuir–Blodgett technique [3]. All peaks in C8H spectrum are blue-shifted by 5–6 cm^{-1} in respect to results for C18H [3]. Blue spectral shift of comparable value was reported to occur with the increase of defects concentration resulting from the shortening of the alkyl chain [23]. Unfortunately our attempt to quantitatively estimate the radio of CH_2 and CH_3 absorbances was hindered by difficulties in the baseline correction procedure. It is seen, that the presence of *trans–gauche* defects leads to appearance of the new peaks in SFG spectrum; their frequencies are known. In respective IR spectrum only the slight shift of existing peaks is observed. Aside from the chain distortion such shift may be induced by the other factors. Thus, SFG has clear advantage over FTIR in reliability of the alkyl chain defects detection.

Wide XPS scans of the C8H monolayer sample and the fused silica substrate with peak assignments are displayed in Fig. 3. The spectra are almost identical and differ mainly in carbon C(1s) peak area, which is 5 times larger for the sample with monolayer. The peak next to Si(2p) was proven to be a device artifact. Results of Bain and Whitesides [28] indicate that electron escape depth in aliphatic monolayers varies quite significantly with kinetic energy. Accordingly, Si(2p) and O(1s) which originate from the substrate and adjacent cross-linked siloxane network should exhibit different attenuation in the monolayer. Thus, SAM film thickness can be estimated by comparison of peak area ratios prior and after SAM deposition. For Mg X-ray source, the kinetic energies of photoelectrons emitted from Si(2p) and O(1s) are 1150 and 720 eV, respectively, and the corresponding electron escape depths in compact aliphatic film according to the published data [28] should be $\lambda_1 = 34$ Å and $\lambda_2 = 21$ Å. The ratio M of Si(2p) and O(1s) intensities is calculated as

$$M = M_0 \exp\left(\frac{d}{\lambda_2} - \frac{d}{\lambda_1}\right) \qquad (2)$$

where d is the film thickness, M_0 is the peaks ratio

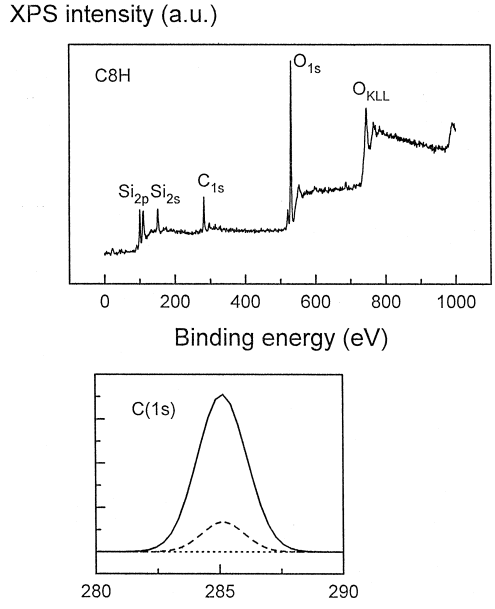

Fig. 3. XPS spectra of fused silica substrate before deposition (top) and the C(1s) region of C8H monolayer on the substrate (bottom) before and after deposition, represented by dashed and solid curves, respectively.

for the substrate without the monolayer. Accounting for possible incomplete surface coverage, we obtain

$$M = M_0 \frac{\theta \exp\left(-\frac{d}{\lambda_1}\right) + 1 - \theta}{\theta \exp\left(-\frac{d}{\lambda_2}\right) + 1 - \theta} \quad (3)$$

where θ is the portion of sample surface, covered with the film. We omit correction for the chain tilt since, as reported by Hoffmann et al. [23], the average tilt angle of hydrocarbon chain in alkylsiloxane monolayers is small with chain axis close to surface normal and is relatively independent on the chain length.

The observed XPS peak positions and relative intensities for our samples are listed in Tables 1 and 2. Given the theoretical layer thickness per CH_2 unit of 1.27 Å [29] one monolayer of C8H has the thickness $d = 10.2$ Å. Using this value and fitting Si(2p) and O(1s) data from the Table 2 to the formula (3) we obtain the surface coverage $\theta = 0.87$. Thus, the deposited self-assembled film is close to a compact monolayer of C8H. This result is in accord with recent AFM studies [8,30], showing that the growth of alkylsiloxane film proceeds via formation of one monolayer thick islands, which later grow in size to form an almost compact monolayer.

It should be noted that our data for Si(2p):O(1s) XPS intensity ratios could also correspond to a surface, incompletely covered with islands thicker than a monolayer. But, by assuming that such islands were composed of just two layers, the calculation would lead to the value of surface coverage as low as 59%. This is in contradiction with previous AFM data [18], which indicated that while formation of multilayer during alkylsiloxane deposition was not excluded, multilayer was formed only after complete monolayer coverage was achieved. From the data of Table 2, it is seen that the intensity ratios of Si(2p) and O(1s) remain the same within 5% accuracy for all samples with deposited monolayers, meaning that all films are about the same thickness and compactness. Thus, O(1s) peak is chosen as a reference for comparison of peak intensities from different samples.

Table 1
XPS peak positions (binding energies in eV)

Sample	$C(1s)^H$	$C(1s)^F$	F(1s)	O(1s)	Si(2p)
C8H	285.1	xxxxxx	xxxxxx	533.5	103.2
C8F	285.5	290.5	689.9	533.5	103.1
Mixed 1:5	285.3	290.9	689.3	533.3	103.0
Mixed 1:8	285.1	291.2	689.9	533.6	103.2
Substrate	285.1	xxxxxx	xxxxxx	533.6	103.3

Table 2
XPS relative peak areas referenced to O(1s)

Sample	$C(1s)^H$	$C(1s)^F$	F(1s)	O(1s)	Si(2p)
C8H	0.1609	xxxxxx	xxxxxx	1	0.2024
C8F	0.0684	0.0598	0.6305	1	0.1939
Mixed 1:5	0.0913	0.0399	0.4302	1	0.2105
Mixed 1:8	0.0954	0.0124	0.1922	1	0.2056
Substrate	0.0344	xxxxxx	xxxxxx	1	0.1743

3.2. Fluorinated samples

The IR spectrum of C8F monolayer, as plotted in Fig. 2 (dashed curve), is rather similar to that of C8H monolayer. Although there are only two (out of 7) methylene groups left in C8F chain, the strengths of both methylene stretches for C8F monolayer are only about 40% less than those for C8H. A residual feature at 2960 cm^{-1} in the spectrum seems to be present still. Part of the observed IR intensity of the methylene stretches can be attributed to the hydrocarbon residues (such as hexadecane, further discussed below) present on the surface.

SFG spectra of C8F monolayer, recorded with different SFG–visible–IR polarization combinations are presented on Fig. 4. Only *ssp*- and *ppp*-polarization combinations appear to yield detectable SFG response. The major peak in both spectra is centered around 2920 cm^{-1}; relevant SFG strengths differ by a factor of two. The *ssp* SFG spectrum of C8F monolayer is depicted in Fig. 5 along with its IR spectrum for comparison. SFG and IR spectrometers were calibrated independently and the coincidence of peak frequencies is not artificial. Therefore, we can assign major SFG peak to antisymmetric methylene stretching mode. The shoulders on both sides of it near 2880, 2935 and 2960 cm^{-1} indicate the presence of methyl containing species. In C8F monolayer, methyl group is fully fluorinated and no methyl vibrations can originate from it. Thus, the IR, SFG

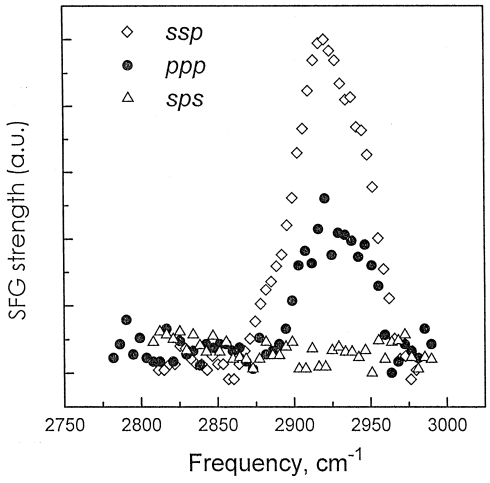

Fig. 4. SFG spectra of C8F monolayer, recorded with *ssp* (open diamonds), *ppp* (solid circles) and *sps* (open triangles) polarization combinations.

and XPS spectra (presented below) show clearly the presence of hydrocarbon residue in the C8F monolayer. It should be noted that the shoulder at 2880 cm^{-1} is not present in the *ppp* spectrum.

The most interesting SFG result is the presence of antisymmetric methylene stretch and the absence of symmetric stretch in the spectra. In the fully symmetric environment C_2H_4 subgroup should have C_{2h} local symmetry and have totally four C–H stretching modes [31]. Because of inversion symmetry and in accord with mutual exclusion rule, two of these C–H stretches (*g*-vibrations) are purely Raman active, while the other two (*u*-vibrations) are purely infrared active [32]. Accordingly, no SFG response from any of these modes should be expected because none of them is simultaneously IR and Raman active. The existence of SFG signal from fluorinated sample at methylene stretching frequency suggests that the symmetry of C_2H_4 group in C8F is lower than C_{2h}.

There are two possible reasons for the symmetry reduction. Charge redistribution induced by fluorination of the alkyl chain may leave two carbon atoms in C_2H_4 subgroup unequal and thus not interchangeable in terms of symmetry. Alternatively, the geometry of this subgroup may be distorted by the influence of the adjacent fluorinated alkyl chain, which is known to have helical [33], rather than flat structure. The simplest case of such distortion may be a twist around C–C bond. In both cases the inversion symmetry of the subgroup is lost and appearance of SFG response may be expected.

In SFG spectrum of C8F, only the antisymmetric CH_2 mode is observed. Thus, only this mode has substantial Raman activity. Both methylene modes in C8F are IR active which is seen from Fig. 2. It follows that the symmetry perturbation induced by fluorination of alkyl chain is such that only the Raman activity of antisymmetric *u*-stretch of the C_2H_4 group is significantly enhanced. Substantial activity of only antisymmetric mode may indicate that some symmetry in C_2H_4 is still present, because in the total absence of symmetry one should expect both methylene vibrations to appear, especially since their IR strengths are comparable (see Fig. 2). On the other hand, in the presence of *trans–gauche* defects in alkyl chain (which could be regarded as a form of chain twist) symmetric methylene stretch dominates over the asymmetric one (see Fig. 1). Thus, the charge redistribution seems to be a more likely mechanism of the induced SFG activity in C_2H_4.

Detailed analysis of SFG spectrum of C8F requires rigorous calculation of the molecular hyperpolarizability. However, even without such analysis it is seen that the spectra of partially fluorinated sample (C8F) and a sample with chain defects (C8H) are clearly different. IR spectroscopy is much less sensitive (see Fig. 2) in detecting such changes. While in SFG spectrum the relative amplitudes of peaks

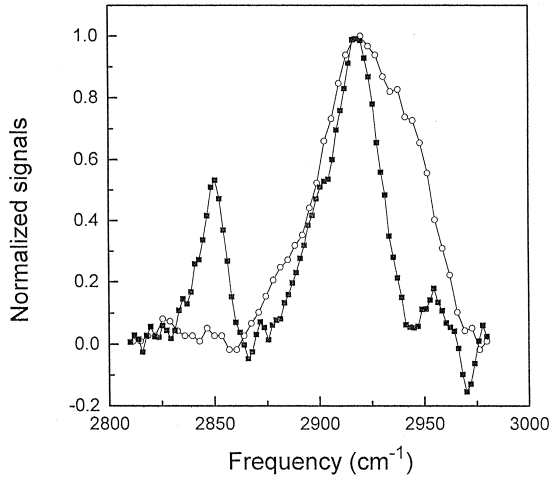

Fig. 5. Comparison of *ssp* SFG (open circles) and IR (solid squares) spectra of pure C8F monolayer.

change drastically after the chain fluorination only slight frequency shifts and bandwidth changes are observed in respective IR spectra. One cannot expect the Raman spectroscopy to be better than IR in this case since the strengths of Raman peaks are not directly related to the presence or absence of the central symmetry. Here, we are dealing with the case where SFG spectroscopy, owing to its specific selection rules, is able to detect the molecular symmetry perturbations and distinguish between different types of them.

In relation to the potential of SFG spectroscopy, we notice here that symmetry distortion may also lead to appearance of the two formerly purely Raman active *g*-modes in SFG spectrum. Some reported results on Raman spectroscopy of alkyl-chain monolayers [34–36] suggest that frequencies of these two modes are different from their IR-active analogs. The presence or absence of SFG response from such modes can provide yet another opportunity to characterize symmetry changes in the molecules under investigation.

The XPS spectrum of C8F layer is depicted in Fig. 6. Compared with the spectrum of C8H sample, new peaks that can be assigned to fluorine transitions

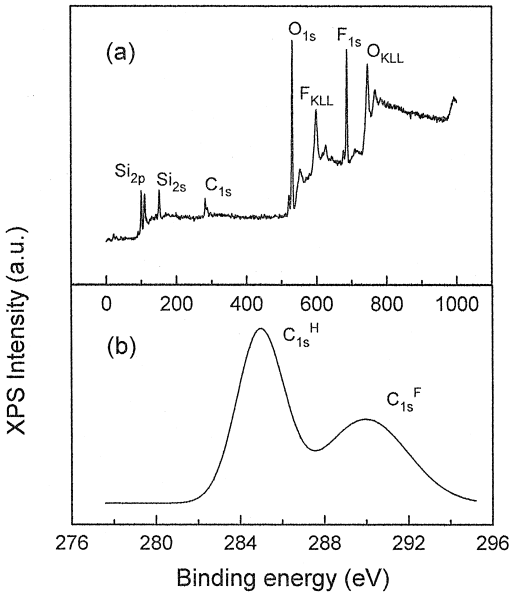

Fig. 6. XPS spectrum of C8F monolayer on fused silica. (a) Survey scan, (b) C(1s) spectrum region.

are present. In addition, the C(1s) emission exhibits a doublet structure with a second peak centering around 290 eV. We attribute this peak to the combined emission from the CF_2 and CF_3 groups in C8F and present the data for hydrogen- and fluorine-bonded carbon in separate columns, designated as $C(1s)^H$ and $C(1s)^F$, respectively. In the XPS study of similar sample performed by Ge et al. [3], the binding energies of CF_2 and CF_3 were reported to be different. In that case, the photoelectrons were detected at an acute angle of 15° from the surface and the measurement was much more sensitive to the surface adsorbate than our measurement at 90°. Thus, the signal contribution from CF_3 group located on top of the monolayer could not be well resolved from that of CF_2 groups in the present study.

3.3. Mixed monolayer samples

The *ssp* SFG spectra of different C8H:C8F mixed samples are presented on Fig. 7. As observed from the graph, the spectra of the samples change continuously from the one characteristic for pure C8H to the one essentially identical to pure C8F, with the increase of fluorinated compound concentration in deposition solution. These results additionally prove that SFG spectral features of fluorinated monolayer are neither an artifact nor the result of sample contamination. It should be noted that the solution with only 40% of fluorinated alkylsilane produces essentially pure fluorinated C8F layer. Further increase of fluorinated alkylsilane concentration does not result in any significant change of SFG spectrum. The relative concentration of the components in the solution and in the monolayer is very different with C8F being adsorbed preferentially. Such behavior in the process of mixed alkylsiloxane monolayers self-assembly was reported before [37].

We have further checked if C8H molecules already adsorbed on the surface can be replaced by C8F molecules in a subsequent dipping. A series of samples were prepared by consecutively dipping the substrate in two pure solutions without intermediate baking and with minimal delay between dippings. With such an arrangement, the monolayer from the first solution was always found to be deposited. Thus, the substitution mechanism seems to be un-

likely to explain the preferential adsorption of fluorinated compound. Consequently, fluorinated octylchlorosilane must have much faster adsorption rate than octyltrichlorosilane. Indeed, Banga et al. [18] have reported that this particular fluorinated chlorosilane forms compact monolayer about 10 times faster than octadecyltrichlorosilane (OTS). Based on this result, the authors concluded that the adsorption rate difference between the two alkylchlorosilanes was 'system inherent', i.e., due to the fluorination of alkyl chain. However, they compared two silanes with different chain lengths which were deposited from the solutions with different residual water content. The latter fact is critical because self-assembly of silanes involves hydrolysis and the deposition rate is dependent on the amount of water present in the system [24]. In our case, two chlorosilanes with identical head groups and chain lengths were concurrently adsorbed from the same solution. Thus, our comparison of fluorinated and non-fluorinated species is more consistent than the one performed by Banga et al. [18]; both results unambiguously demonstrate that alkyl chain fluorination considerably accelerates self assembly of amphiphiles.

It is possible to argue that the observed adsorption imbalance could be induced by the higher concentration of fluorinated compound near the free surface of the solution. In such case, fluorinated species could be preferentially adsorbed just by being the first to come in contact with the substrate surface in the dipping process. However, experiments [18] show, that under comparable conditions a half-monolayer coverage of fluorinated alkylsiloxane is achieved after about 20 seconds of deposition. This result indicates that any considerable adsorption of fluorinated compound is unlikely to happen during the dipping stage which in our experiments was less than 1 s.

It is readily seen (cf. two graphs at the bottom of Fig. 7) that both methylene stretch peaks arising most likely from *trans–cis* (*–gauche*) defects, almost disappear with addition of a relatively small amount of fluorinated species to C8H monolayer. In fact, no other structural changes in SFG spectrum are observed at this step. Such influence is an evidence of chain–chain interaction in mixed samples which is possible only if significant amounts of both species

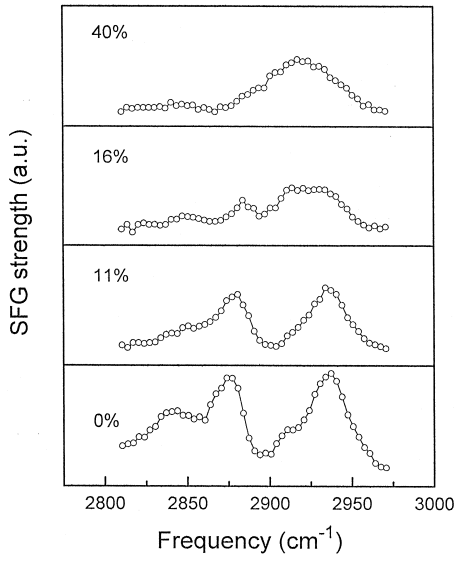

Fig. 7. SFG spectra of mixed C8F + C8H monolayers, deposited with different content of fluorinated compound in the solution (indicated by %).

are closely coadsorbed. In contrast to that, previously described Langmuir–Blodgett film of similar mixed composition [3] was found to consist of well-separated macroscopic regions with relatively pure content of either species. In our case while the layer structure may be island-like, a substantial number of islands consist of the mixture of two different compounds.

A model was proposed (see [25] and references therein), according to which self-assembly of alkylsilanes involves formation of LB-like film on top of the water layer present at the substrate surface. During deposition such film reorganizes into certain 2D phases by surface diffusion, cross-links forming intermolecular siloxane bonds and finally is anchored to the surface. Surface diffusion and structural relaxation result in equilibrium phases formation, while cross-linking tends to freeze the film inhibiting reorganization. The final structure of the SAM is defined by this competition and depends on the chain length and deposition temperature. If we apply this model to self-assembly of two different silanes from a mixed solution, surface diffusion must lead to phase segregation, while cross-linking should prevent it. Thus, the observation of close coadsorption suggests

that at least for the mixed film cross-linking is relatively faster process than the surface diffusion. Most likely it is C8F that is responsible for such behavior. This assumption is in accord with fast self-assembly of fluorinated species observed by Banga et al. [18]; however, the reason seems to be not only faster hydrolysis rate, but also faster cross-linking. Both these factors arise from higher chemical activity of silane head group induced by alkyl chain fluorination. Charge redistribution in C_2H_4 subgroup of C8H detected by SFG is another evidence of such influence.

Adding fluorinated molecules with more rigid chains into C8H monolayer seems to help eliminating defects in the latter. This effect could be useful for decreasing the concentration of chain defects and thus increasing ordering of non-fluorinated monolayers. Defects concentration is decreased despite the fact that fast cross-linking induced by adding C8F can freeze the film structure on the early disordered stage. Thus C8F chain seems to be more rigid, less likely to develop quirks and capable of straightening its neighbors. Further increase of C8F content (two top graphs of Fig. 7) leads to reappearance of antisymmetric methylene stretch peak which to certain extent may serve as a measure of C8F content in the monolayer.

Additional evidence of close coadsorption of C8H and C8F arises from the fact that SFG spectra of mixed samples cannot be reconstructed by combining the spectra of pure monolayers. Fig. 8 shows the comparison between experimental SFG intensity spectrum of mixed 1:5 monolayer and reconstructed one (open circles and solid curve, respectively). The reconstructed spectrum was obtained using the following formula:

$$I_{\mathrm{mix}} = |W_{\mathrm{C8H}}\,\chi^{(2)}_{\mathrm{C8H}}(\omega) + W_{\mathrm{C8F}}\,e^{i\alpha}\chi^{(2)}_{\mathrm{C8F}}(\omega) + \chi^{(2)}_{\mathrm{nr}}|^2 \tag{4}$$

Here, W_{C8H}, W_{C8F} are relative weights and α is the relative phase of two complex susceptibilities $\chi^{(2)}_{\mathrm{C8H}}$ and $\chi^{(2)}_{\mathrm{C8F}}$. Complex term $\chi^{(2)}_{\mathrm{nr}}$ reflects non-resonant background contribution. The profiles of $\chi^{(2)}_{\mathrm{C8H}}(\omega)$ and $\chi^{(2)}_{\mathrm{C8F}}(\omega)$ are derived by deconvoluting SFG spectra of pure C8H and C8F into Lorentzian components according to the formula (1). Weights W_{C8H} and W_{C8F} phase difference a are then adjusted to produce the best fit of experimental mixed monolayer spectrum. Non-resonant term $\chi^{(2)}_{\mathrm{nr}}$ was also adjusted during both deconvolution and reconstruction stage, but was found to be negligibly small. Fitting was performed under the assumption that the C–H stretching frequencies of the stray hydrocarbons (if present) coincide with the relevant frequencies in alkylsiloxanes. This assumption does not affect the quality of the fit and allows for automatic account for the stray hydrocarbons contribution which becomes included in $\chi^{(2)}(\omega)$ profile.

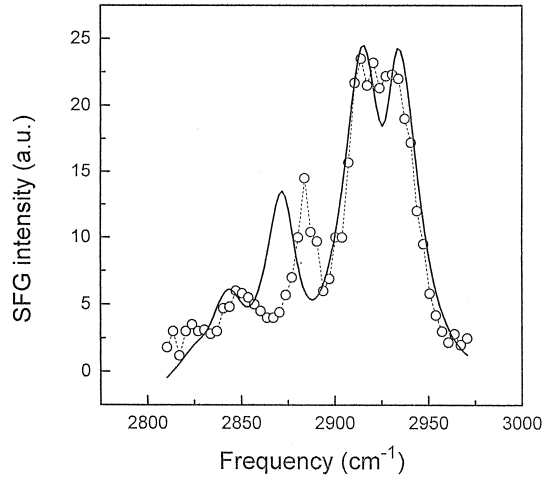

Fig. 8. C8F:C8H mixed monolayer with 1:5 component ratio during deposition. Experimental SFG spectrum (open circles) and one reconstructed from pure C8H and C8F SFG spectra (solid curve).

A reasonably good fit can be achieved for overlapped peaks of antisymmetric methylene and Fermi resonance of symmetric methyl stretches at 2920 and 2940 cm^{-1}, respectively. However, no combination of adjustable parameters was found to simultaneously eliminate noticeable discrepancy between the values of methyl symmetric stretching frequency in experimental and reconstructed spectra around 2880 cm^{-1}. Thus, the reproduction of the three strongest mode amplitudes was used as a criterion for the fit. Such fit gives an estimate of 70% for relative C8F content. We note here, that contrary to the case of conventional IR spectroscopy, SFG signals are coherent and interference terms affect the lineshape of the peaks. In particular, observed peak frequency could be shifted by interference with either the wing of the adjacent peak or with the SFG signal generated in the substrate. Nevertheless, even the combi-

nation of these two factors cannot compensate for the frequency shift of methyl symmetric stretch observed in our case. Thus, we ascribe this shift to the influence of C8F on coadsorbed C8H.

XPS data from the mixed samples are also summarized in Tables 1 and 2. Comparison of the fluorine contents in the two mixed samples with pure C8F sample yields the following results. For 1:5 sample (ratio of fluorinated and non-fluorinated silane concentrations in the solution), the F(1s) peak area normalized by O(1s) shows the relative fluorine content in the mixed sample to be 68% of pure fluorinated monolayer. Comparison of fluorine-bonded C(1s) peak at 289 eV for 1:5 sample with that of pure C8F sample gives the relative fluorine content of 67%, i.e., essentially the same as one derived directly from F(1s) peak ratio. This value is also consistent with the 70% estimate, derived for the 1:5 sample from the fit of combined SFG spectra for the pure C8H and C8F (Fig. 8). The corresponding number obtained from the amplitude of antisymmetric methylene stretch in SFG spectrum is 56%. The latter result cannot be accepted as accurate since as it was noted previously, the strength of antisymmetric methylene stretch is not an exact measure of fluorine content. Thus, it is concluded that within experimental error, the 1:5 sample actually contains about 70% fluorinated species in the adsorbed monolayer.

Similar comparison for the 1:8 sample with pure fluorinated one gives relative fluorine content being 30% from F(1s) ratio, 21% from C(1s) ratio and 17% from antisymmetric methylene stretch in SFG spectra. For this sample the fit of SFG spectrum with the spectra of pure C8H and C8F cannot be performed reliably since methylene antisymmetric stretch is very weak. The increased discrepancy of the XPS data is obviously due to the low signal strengths of C8F peaks. Content of C8F for 1:8 sample is thus about 25%. The estimate derived from methylene SFG strength is again somewhat lower than one given by XPS.

C(1s) peak areas for pure C8F and 1:5 samples appear to be the same, indicating that no significant variation in the degree of surface coverage exists. The ratio of C(1s) peaks in the doublet structure should reflect the concentration ratio of fluorine- and hydrogen-bonded carbon atoms. Taking into account the number of such atoms in C8F chain, one should expect this ratio to be $R_1 = 3$ for pure and $R_2 = 1.01$ for 1:5 sample, respectively; the latter number being based on 70% fluorine content. However, the experimental values are $R_1 = 0.87$ and $R_2 = 0.44$, respectively. The observed ratio $R_1/R_2 = 1.98$ is also much lower than the calculated value, which should be almost 3. The calculation strongly suggests a higher relative content of hydrogen-bonded carbon than the SAM alone can provide. Namely, hydrocarbon species other than C8H and C8F must be adsorbed on the substrate in substantial amounts.

Assuming that there exists a significant hydrocarbon residue in all samples, we can easily show that the experimental values of R_1 and R_2 for C8F, 1:5 and 1:8 samples can be satisfactorily explained by adding species with five to six additional hydrogen-bonded carbon atoms per each adsorbed monolayer molecule. Such residual hydrocarbon species may also give rise to methyl resonances observed in the SFG spectrum of C8F, provided the residue molecules exhibit sufficient degree of ordering. We note that residual hydrocarbons are unlikely to contribute to the methylene stretch signal since its intensity decreases along with the decrease of C8F contents almost to zero while the residue concentration remains unchanged.

The most likely source of the residue is hexadecane used as a solvent during monolayer deposition. To verify this assumption, we have compared XPS spectra of freshly ozone-oxidized fused silica with that of a similar sample, but dipped into hexadecane and washed by standard procedure before placing it into XPS chamber. It is observed that the deliberately solvent-contaminated sample exhibits a C(1s) intensity about 2.4 times stronger than that of the control sample. Furthermore, the total C(1s) signal strength is about one half of that for C8H layer. This number is consistent with the amount of hydrocarbon residue, derived from R_1 and R_2 ratios (5 residual aliphatic carbons per 8 carbon atoms of C8F). Based on the analysis of R_1 and R_2 for C8F and mixed samples, SFG spectra and the results of the solvent experiment, we can conclude that there is significant coadsorption of solvent molecules along with the SAM on the substrate.

Earlier studies have shown that hexadecane and similar linear alkanes can be easily incorporated into the incompact monolayer [38,39]. Geometrical simi-

larities between the solvent and monolayer molecules were found to be a key factor for such incorporation [40]. Comparison of OTS monolayers deposited from hexadecane and toluene solutions by ellipsometry, XPS and FTIR as performed by Kallury et al. [41], indicated that hexadecane was intercalated between the molecules of the SAM and not just physisorbed on top of it. Our results for monolayers with comparatively short chain length of eight carbon atoms also show hexadecane coadsorption, albeit of somewhat lower level (one molecule of hexadecane per ca. 3 silane molecules). The amount of coadsorbed hexadecane is found to be similar in pure fluorinated and mixed films. This suggests that hexadecane is equally well entrapped among both aliphatic chains and their fluorinated analogs. Helical structure of $-CF_2-$ chains [33] appears to impose no obstacles for hexadecane retention. Apparently the vacancies formed among the thicker $-CF_2-$ chains are readily occupied by hexadecane despite poor geometrical fit between the flat and the helical chain structures. The adsorption of hexadecane in the form of overlayer seems unlikely, especially in the case of C8F monolayer, since its surface consists of closely packed CF_3 groups and thus should be highly oleophobic. This was demonstrated previously [42] even for closely packed non-fluorinated monolayers.

In contrast to the case of OTS/hexadecane film, relatively long entrapped hexadecane molecules should substantially protrude out of C8H/C8F monolayer. This should make our monolayers less oleophobic, compared to either perfect (no retained hexadecane) or OTS/hexadecane monolayer. Oleophobicity is decreased whenever the layer of terminating methyl groups becomes less compact, e.g., due to the presence of chains with different lengths in the monolayer [43]. In accord with this assumption we have found the hexadecane contact angle of our C8H film to be about 35–40°, which is somewhat lower than the typical value of 45–48° reported for OTS film deposited from hexadecane solution [42]. Similar difference is observed for contact angles with water, namely 105° vs. 115°.

4. Conclusions

We have successfully prepared mixed fluorinated/non-fluorinated alkylsiloxane monolayers on the surface of fused silica by self-assembly deposition technique. SFG, FTIR and X-ray photoemission spectroscopies provide a consistent picture of the system under investigation. In mixed monolayers, different species are closely coadsorbed and influence each other. Furthermore, the vibrational spectroscopic data for mixed samples are not the simple linear combination of those for the pure samples; frequencies of several vibrational modes shift due to coadsorption. In this respect, mixed self-assembled films differ from Langmuir–Blodgett monolayers of similar composition, where different species segregate into separate phases. The surface mobility of the studied siloxanes during self-assembly is limited which prevents phase separation in the film.

SFG vibrational spectroscopy in the C–H stretching region is shown to be not only a convenient tool for distinguishing different monolayers and estimating their abundances on the surface, but also capable of detecting adsorbed alkyl chain distortions. Such distortions are not revealed by IR transmission spectroscopy.

We have found that the competitive self-assembly of fluorinated chlorosilane and its non-fluorinated analog with the same chain length and identical headgroup results in preferential adsorption of the fluorinated compound. It is shown that the major reason for the observed adsorption imbalance is alkyl chain fluorination.

The residue of the organic solvent such as hexadecane used in the process of self-assembly was found in prepared monolayers. No major difference in the amount of solvent residue in all investigated monolayers is observed. In particular, solvent incorporation in fluorinated alkylsiloxane SAM is reported for the first time. Surface concentration of the residue may be as high as 30% of the monolayer.

Acknowledgements

The authors wish to acknowledge the partial support of the work from National Science Council of R.O.C. under the grants NSC 85-2113-M-001-032, NSC-85-2112-M-001-030 and NSC 83-0208-M009-069.

References

[1] H. Zarrad, J.M. Chovelon, P. Clechet, N. Jaffrezic-Renault, C. Martelet, M. Belin, H. Perez, Y. Chevalier, Sensors Actuators A 46-47 (1995) 598.
[2] A. Ulman, An Introduction To Ultrathin Organic Films: From Langmuir–Blodgett to Self-Assembly, Academic Press, San Diego, 1991.
[3] S. Ge, A. Takahara, T. Kajiyama, J. Vac. Sci. Technol. A 12 (1994) 2530.
[4] H.G. Linde, R.T. Gleason, J. Polymer Sci.: Polymer Chem. Edn. 22 (1984) 3043.
[5] S.R. Wasserman, Y.-T. Tao, G.M. Whitesides, Langmuir 5 (1989) 1074.
[6] S.R. Cohen, R. Naaman, J. Sagiv, J. Phys. Chem. 90 (1986) 3054.
[7] S.R. Wasserman, G.M. Whitesides, I.M. Tideswell, B.M. Ocko, P.S. Pershan, J.D. Axe, J. Am. Chem. Soc. 111 (1989) 5852.
[8] D.K. Schwartz, S. Steinberg, J. Israelashvili, J.A.N. Zasadzinski, Phys. Rev. Lett. 69 (1992) 3354.
[9] I. Haller, J. Am. Chem. Soc. 100 (1978) 8050.
[10] J. Sagiv, J. Am. Chem. Soc. 102 (1980) 92.
[11] X. Xiao, J. Hu, D.H. Charych, M. Salmeron, Langmuir 12 (1996) 235.
[12] Y.L. Chen, C.A. Helm, J.N. Israelashvili, J. Phys. Chem. 95 (1991) 10736.
[13] P.G.D. Gennes, Rev. Mod. Phys. 57 (1985) 827.
[14] L.-K. Chau, M.D. Porter, Chem. Phys. Lett. 167 (1990) 198.
[15] C.A. Alves, M.D. Porter, Langmuir 9 (1993) 3507.
[16] M. Fujii, S. Sugisava, K. Fukada, T. Kato, T. Shirakawa, T. Semiya, Langmuir 10 (1994) 984.
[17] H. Tada, H. Nagayama, Langmuir 10 (1994) 1472.
[18] R. Banga, J. Yarwood, A.M. Morgan, B. Evans, J. Kells, Langmuir 11 (1995) 4393.
[19] X.D. Zhu, H. Suhr, Y.R. Shen, Phys. Rev. B 35 (1987) 3047.
[20] J.H. Hunt, P. Guyot-Sionnest, Y.R. Shen, Chem. Phys. Lett. 133 (1987) 189.
[21] Y.R. Shen, Nature 337 (1989) 519.
[22] P. Guyot-Sionnest, J.H. Hunt, Y.R. Shen, Phys. Rev. Lett. 59 (1987) 1597.
[23] H. Hoffmann, U. Mayer, A. Krischanitz, Langmuir 11 (1995) 1304.
[24] M.E. McGovern, K.M.R. Kallury, M. Thompson, Langmuir 10 (1994) 3607.
[25] A.N. Parikh, D.L. Allara, I.B. Azouz, F. Rondelez, J. Phys. Chem. 98 (1994) 7577.
[26] P. Guyot-Sionnest, R. Superfine, J.H. Hunt, Y. R Shen, Chem. Phys. Lett. 144 (1988) 1.
[27] J.Y. Huang, Y.R. Shen, Advanced Ser. Phys. Chem. 5 (1995) 31–35.
[28] C.D. Bain, G.M. Whitesides, J. Phys. Chem. 93 (1989) 1670.
[29] C.D. Bain, E.B. Troughton, Y.-T. Tao, J. Evall, G.M. Whitesides, R.G. Nuzzo, J. Am. Chem. Soc. 111 (1989) 321.
[30] K. Bierbaum, M. Grunze, A.A. Baski, L.F. Chi, W. Shrepp, H. Fuchs, Langmuir 11 (1995) 2143.
[31] S. Krimm, C.Y. Liang, G.B.B.M. Sutherland, J. Chem. Phys. 25 (1956) 549.
[32] K. Nakamoto, Infrared Spectra of Inorganic and Coordination Compounds, 3rd edn., Wiley, New York, 1978, p. 26.
[33] R.E. Moynihan, J. Am. Chem. Soc. 81 (1959) 1045.
[34] R.G. Snyder, S.L. Hsu, S. Krimm, Spectrochimica Acta 34 A (1978) 395.
[35] M.A. Bryant, J.E. Pemberton, J. Am. Chem. Soc. 113 (1991) 3629.
[36] M.A. Bryant, J.E. Pemberton, J. Am. Chem. Soc. 113 (1991) 8284.
[37] Y.-T. Tao, D.-Y. Huang, Bull. Inst. Chem., Acad. Sinica 35 (1988) 23, also private communication.
[38] L.S. Bartell, R.J. Ruch, J. Phys. Chem. 60 (1956) 1231.
[39] L.S. Bartell, R.J. Ruch, J. Phys. Chem. 63 (1959) 1045.
[40] J.H. Kim, T.M. Cotton, R.A. Uphaus, Thin Solid Films 160 (1988) 389.
[41] K.M.R. Kallury, M. Thompson, C.P. Tripp, M.L. Hair, Langmuir 8 (1992) 947.
[42] J. Gun, J. Sagiv, J. Colloid Interface Sci. 112 (1986) 457.
[43] V.J. Schaefer, J. Phys. Chem. 45 (1941) 681.